Available online at www.sciencedirect.com
SCIENCE DIRECT®
Talanta 67 (2005) 492–497
Talanta
www.elsevier.com/locate/talanta

Synthesis of polystyrene beads loaded with dual luminophors for self-referenced oxygen sensing

Sang Hyuk Im [a,1], Gamal E. Khalil [a,1], James Callis [a], Byung Hyun Ahn [b], Martin Gouterman [a], Younan Xia [a,*]

[a] *Department of Chemistry, University of Washington, Seattle, WA 98195-1700, USA*
[b] *Division of Materials Science and Engineering, Pukyong National University, Yongdang-Dong Nam-Ku, 608-739 Busan, South Korea*

Available online 1 August 2005

Abstract

Dispersion polymerization has been successfully applied to synthesize monodisperse polystyrene beads loaded with SiOEP and PtOEP for self-referenced oxygen sensing. The polystyrene beads became larger in size as the concentration of initiator was increased due to the reduction of primary particles precipitated from the polymerization medium. The dual luminophors showed similar absorption spectra but two distinctive emission spectra with peaks at 580 and 650 nm for SiOEP and PtOEP, respectively. While the emission of SiOEP exhibited no response to oxygen, the luminescence intensity of PtOEP was monotonically dependent on the concentration of oxygen. From the Stern–Volmer plot, we observed a linear correlation between the intensity ratio of SiOEP at 580 nm to PtOEP at 650 nm and the concentration of oxygen, which could be used to reliably monitor the partial pressure of oxygen in a system.

Keywords: Oxygen sensors; Polystyrene beads; Dual luminophors; Silicon octaethylporphyrin; Platinum octaethylporphyrin; Dispersion polymerization

1. Introduction

Colloidal particles derivatized with luminescent dyes have been exploited for monitoring the concentration of dissolved oxygen in biomedical applications because of their fast response to localized oxygen [1,2]. Recently, Abe et al. have also demonstrated that air-born microspheres loaded with pressure-sensitive dyes could be used to simultaneously acquire the images of both velocity and pressure fields because these particles were sufficiently small to accurately follow the fluid flow and showed the potential for monitoring a two-dimensional pressure field [3]. In spite of these proof-of-concept demonstrations, the reliability of these optical sensing techniques still needs to be improved before they can find use in practical applications. For instance, it has been shown that the detected luminescent signal was strongly dependent on experimental parameters that include the temperature, the light source, the schemes for both illumination and detection, the index of refraction of the medium, and the concentration of dye. These problems can, in principle, be solved by incorporating two different types of luminophors into the colloidal particles, with one serving as the reference and the other for sensing oxygen [1]. In an ideal system, the luminescent dyes should be selected such that both of them have similar response to the experimental parameters (e.g., temperature) while the reference dye will not be quenched by oxygen and the sensing dye will strongly respond to the change of oxygen concentration [4].

To date, oxygen-sensitive luminophors have been mixed with binders and mainly fabricated in the form of thin films or porous films on the surfaces of certain objects in order to measure the concentration of oxygen [5]. For example Rosenzweig et al. incorporated a ruthenium complex in liposomes and explored their use for noninvasive oxygen sensing [2]. Abe et al. have reported on the synthesis of porous silica particles soaked with another ruthenium complex as the oxygen sensor albeit their particles were not uniform in size [3]. From the viewpoint of applications, it would be

* Corresponding author. Fax: +1 206 685 8665.
E-mail address: xia@chem.washington.edu (Y. Xia).
[1] These two authors contributed equally to this study.

0039-9140/$ – see front matter © 2005 Elsevier B.V. All rights reserved.
doi:10.1016/j.talanta.2005.06.046

advantageous to introduce dual luminophors into monodisperse polymer latexes. For instance, such a particle can serve as a micrometer-sized sensor for oxygen detection by capturing the luminescence image with a CCD camera. Such particles can also be dispersed in space to simultaneously monitor the oxygen changes at different locations. Here we report the synthesis of such colloidal particles by incorporating octaethylporphyrin (SiOEP) and platinum octaethylporphyrin (PtOEP) (both are chemically stable) into polystyrene (PS) beads during dispersion polymerization. When loaded with dual luminophors, the PS beads could still be prepared as monodisperse samples and their diameters could be readily varied from 0.5 to 2.6 μm by adjusting the concentration of initiator from 6 to 24 mM.

2. Experimental

2.1. Synthesis of monodisperse PS beads loaded with dual luminophors

In a typical synthesis, 45 mL of ethanol and 5 mL of deionized water (18 MΩ) were placed in a three-neck flask (100 mL) equipped with a condenser. The solution was heated at 80 °C for 30 min and then 0.4 g of poly(vinyl pyrrolidone) (PVP, M.W. ≈ 55,000, Aldrich, the steric stabilizer), 0.009 g of SiOEP (Frontier Scientific), 0.031 g of PtOEP (Frontier Scientific), 5 mL of styrene (Aldrich, the monomer), and 0.1 g (12 mM) of 2,2′-azobisisobutyronitrile (AIBN, Aldrich, the initiator) were sequentially added to the solution. The polymerization was allowed to proceed for 24 h at 80 °C and magnetic stirring was applied during the entire synthesis. Finally, the suspension of PS beads was cooled down to room temperature. The monodisperse polymer beads loaded with SiOEP and PtOEP were collected via centrifugation at 3900 rpm for 2 min, followed by washing with ethanol three times. To vary the size of PS beads loaded with dual luminophors, we altered the amount of AIBN from 0.1 to 0.05 g (6 mM) and 0.2 g (24 mM), respectively, while other conditions were maintained the same.

2.2. Characterization of polymer beads

Samples for SEM studies were prepared by dropping suspensions of the beads on a piece of silicon wafer, followed by drying in a fume hood. SEM images were taken using a field emission scanning electron microscope (FEI-SEM, Sirion XL) operated at an accelerating voltage of 5 kV. Optical micrographs of the PS beads were obtained using a Zeiss Axiovert 200 inverted microscope. The fluorescent images were captured with a Panasonic Industrial Color CCD camera (model number GP-KR222) by acquiring the luminescent light passing through a cutoff filter of 455 nm. The PS beads were excited by a 100-W mercury short arc lamp equipped a band pass filter centered at 405 nm and a line width of 40 nm. The oxygen sensitivities of the PS beads were measured using the set-up (the PMT survey apparatus) described by Harris [6]. Both PtOEP and SiOEP were excited by the light passing through a band pass filter of 400 nm and the emission spectra were recorded from the light passing through a band pass filter of 650 nm for PtOEP and 580 nm for SiOEP, respectively. The samples were surrounded by a gaseous environment whose oxygen concentration was varied from 0 (pure nitrogen) to 21% (air).

3. Results and discussion

For dispersion polymerization, the size of particles is strongly dependent on a number of parameters that include the concentration of initiator, steric stabilizer, or monomer; the polarity of reaction medium; and the polymerization temperature. Among all these parameters, it is most convenient and effective to control the size of particles by adjusting the concentration of initiator or steric stabilizer while maintaining the other variables. In the present study, we controlled the size of PS beads loaded with dual luminophors by varying the concentration of AIBN exclusively. AIBN is an initiator added to the polymerization medium along with the monomer. Fig. 1A shows a typical SEM image of PS beads loaded with SiOEP and PtOEP, which were synthesized with 6 mM AIBN. This image indicates that the PS beads were mainly characterized by two different diameters: ∼560 nm (the majority, >90%) and ∼200 nm (<10%). The small particles could be easily separated from the sample through centrifugation. The small particles seem to originate from a second round of nucleation of the unreacted monomers due to the presence of initiator at a relatively low concentration. To alter the size of PS beads, we increased the concentration of AIBN from 6 to 12 and 24 mM and typical SEM images of these products are given in Fig. 1B and C. These images clearly indicate that the diameters of resultant PS beads had increased to ∼1 and ∼2.6 μm, respectively. The dependence of particle size on the concentration of AIBN is plotted in Fig. 1D, indicating that the PS beads were monotonically enlarged as the concentration of initiator was increased. Our explanation of this finding is as follows. The increase of initiator concentration led to the formation of more free radicals in the medium, which then resulted in shorter polymer chains that were more soluble in the polymerization medium. Because the number of insoluble, long chains was reduced, fewer primary particles were precipitated from the reaction medium and the precipitated particles could grow larger sizes by consuming all of the monomers [7–10]. As the PS bead became larger, their size distribution was also slightly broadened.

Fig. 2A shows a typical optical microscopy image of PS beads (1.0 μm in diameter) containing dual luminophors. These monodisperse particles readily assembled into a hexagonal lattice when their suspension was dropped on the surface of a glass substrate and dried under ambient conditions. Fig. 2B gives a luminescence microscopy image clearly indi-

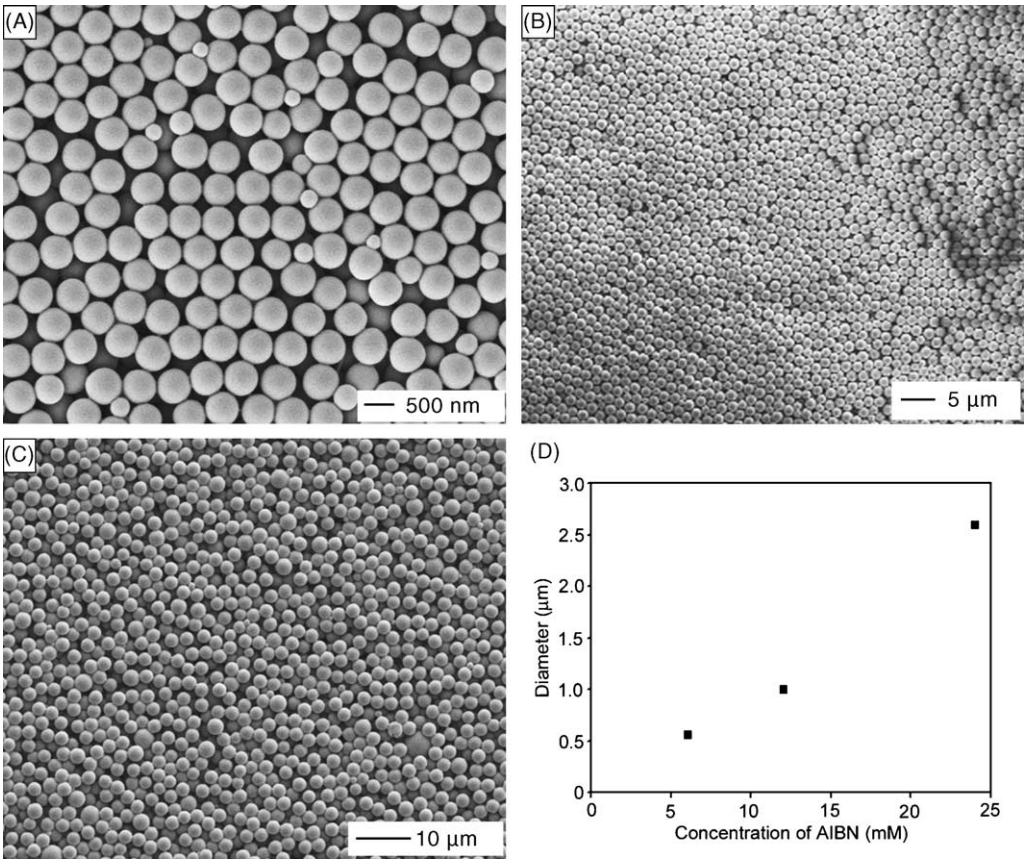

Fig. 1. (A–C) SEM images of PS beads containing SiOEP and PtOEP that were synthesized with different AIBN concentrations: (A) 6 mM, (B) 12 mM and (C) 24 mM. (D) Correlation between the mean diameter of each sample and the concentration of AIBN.

cating the successful incorporation of luminophors into the PS beads. Because the luminescence emitted from the dual luminophors was so bright, it is difficult to distinguish adjacent particles in the hexagonally ordered array. It is believed that the dyes were well-dispersed within the PS beads since the luminescence from each particle appeared to be homogeneous. The arrow indicates an individual PS bead that was emitting strong luminescence, implicating that we can monitor the concentration of oxygen in a certain system by measuring the intensity of luminescence from a single particle.

Fig. 3 shows the emission spectra recorded from PS beads (1.0 μm in diameter) that were loaded with SiOEP and PtOEP. Because the maximum absorption of PtOEP and SiOEP occurred around 400 nm, the sample was excited at this wavelength. It is clear that the emission peaks from these two dyes were distinctively separated and thus each emission could be easily resolved by introducing an appropriate band pass filter. The dashed curve shows the spectrum acquired under pure nitrogen. The emission peaks at 580 and 650 nm corresponded to fluorescence from SiOEP and phosphorescence from PtOEP, respectively. The difference in emission intensity was mainly determined by the molar ratio between SiOEP and PtOEP (1:3 for the present sample) incorporated into the PS beads. The solid curve shows the emission spectrum recorded from the same sample of PS beads under air (with 21% oxygen). Note that the intensity of emission peak at 580 nm from SiOEP was insensitive to the presence of oxygen while the intensity of emission at 650 nm from PtOEP was greatly quenched due to the presence of oxygen. This result implies that the concentration of oxygen can be simply measured by comparing the intensities of peaks emitted from PtOEP and SiOEP dyes loaded into the PS beads.

The quenching of luminescence by oxygen was first discussed by Stern and Volmer for the collision quenching of luminescence in vapor [11]. On the basis of luminescence quenching by oxygen, we can quantitatively monitor oxygen through the Stern–Volmer equation [4,11]:

$$K = k_{\mathrm{nat}} + k_{\mathrm{d}} + k_{\mathrm{q}}[\mathrm{O_2}] = \tau^{-1} \quad (1)$$

Here K is the experimentally observed rate constant of luminescence decay, k_{nat} is the natural radiative decay rate constant, k_{d} is the radiationless decay rate constant, k_{q} is the quenching rate constant by oxygen, and $[\mathrm{O_2}]$ is the molar concentration of oxygen. The reciprocal of K is the emission lifetime, τ. Since the intensity (I) of measured phosphorescence under fixed conditions of illumination and detection is directly proportional to the quantum yield, the quenching of phosphorescence from PtOEP by oxygen can be described by the Kavandi equation [5]. In this case, the observed phospho-

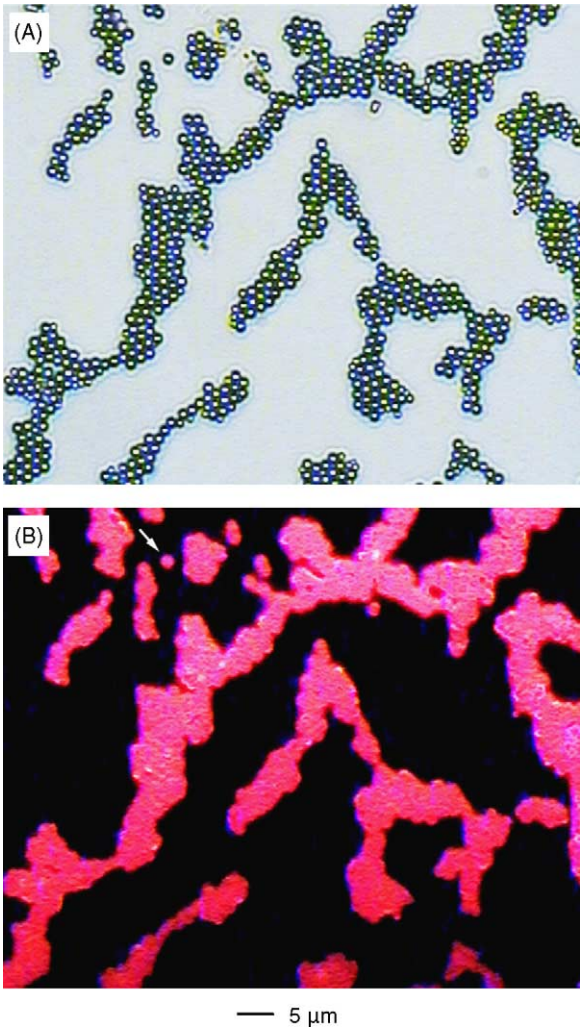

Fig. 2. Optical microscopy images of PS beads (1.0 μm in diameter) that had been loaded with SiOEP and PtOEP: (A) dark field micrograph and (B) luminescence micrograph. The images were taken from the same region of a sample at the same magnification. The arrow indicates a single PS bead.

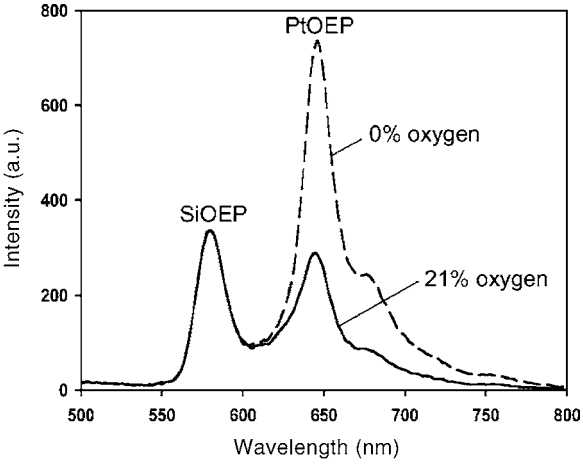

Fig. 3. Emission spectra recorded from PS particles (1.0 μm in diameter) that contained SiOEP as a reference dye and PtOEP as a dye for oxygen sensing. The sample was excited with a light source at 400 nm and under pure nitrogen (no oxygen) and air (21% oxygen), respectively.

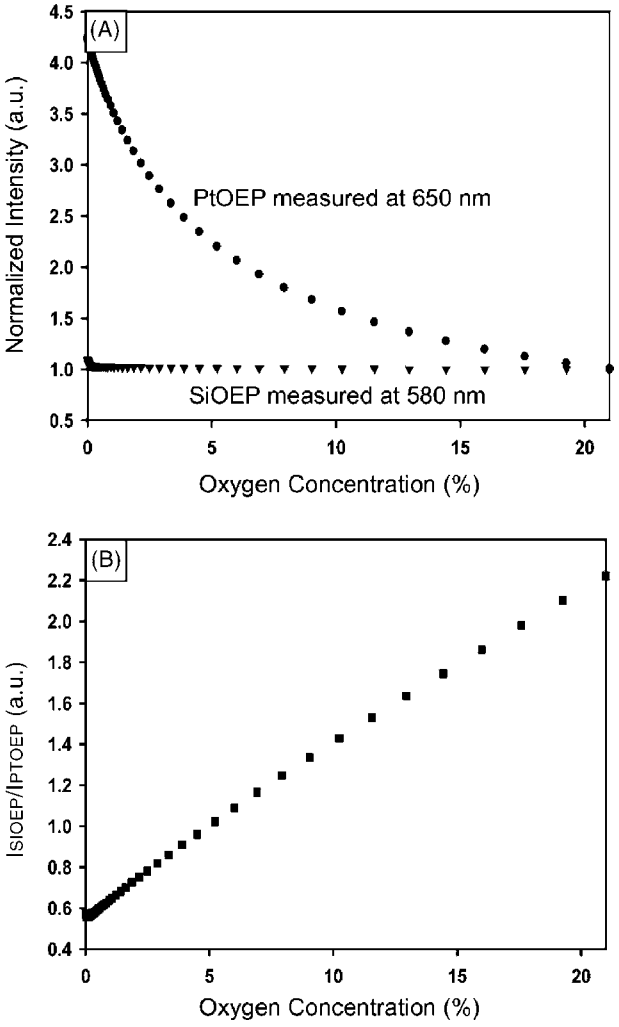

Fig. 4. (A) Oxygen sensitivity of PS beads (1.0 μm in diameter) that were loaded with dual luminophores. The normalized emission intensities were measured at 580 nm for SiOEP and 650 nm for PtOEP. (B) A plot showing the linear dependence between the intensity ratio of SiOEP to PtOEP and the concentration of oxygen.

rescence intensity is inversely proportional to the concentration of oxygen:

$$\frac{I_0}{I} = A + B\left(\frac{[O_2]}{[O_2]_0}\right) \quad (2)$$

where I is the phosphorescence intensity at $[O_2]$; I_0 is the phosphorescence intensity at a reference concentration, $[O_2]_0$. A and B are Kavandi parameters, $A = (k_{nat} + k_d)/(k_{nat} + k_d + k_q[O_2]_0)$, and $B = k_q[O_2]_0/(k_{nat} + k_d + k_q[O_2]_0)$, and both of them can be determined experimentally by plotting I_0/I versus $[O_2]/[O_2]_0$.

Fig. 4A shows how the luminescence intensity of each dye varied as a function of oxygen. As expected, the luminescence from SiOEP (at 580 nm) did not show any change in intensity as the concentration of oxygen was increased from 0 to 21%. In comparison, the intensity of luminescence from PtOEP (at 650 nm) was significantly reduced as the concentration of oxygen was increased (the intensity was inversely

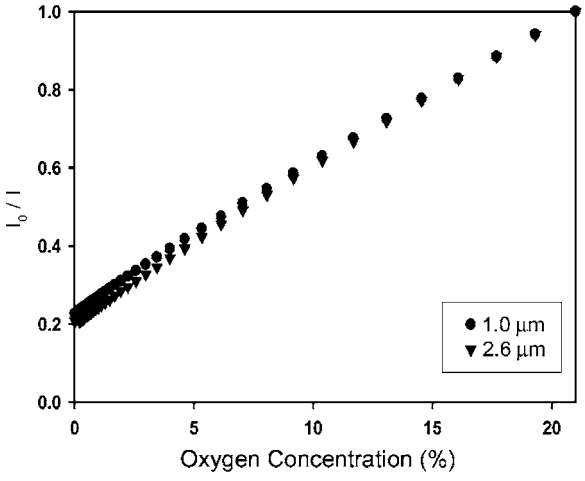

Fig. 5. A comparison between the oxygen Stern–Volmer plots for PS beads of two different sizes: 1.0 and 2.6 mm in diameter.

proportional to the concentration of oxygen). The intensity ratio of SiOEP to PtOEP (I_{SiOEP}/I_{PtOEP}) is plotted as function of oxygen concentration in Fig. 4B. The plot could be fitted to a linear relationship with an intercept of $A = 0.082$, a slope of $B = 0.56$, and a correlation coefficient of $R^2 = 0.998$. Once A and B have been determined, the oxygen concentration can be readily derived from the measured intensity ratio (I_{SiOEP}/I_{PtOEP}).

We also evaluated the influence of size of PS beads on their performance as oxygen sensors. Fig. 5 compares the Kavandi–Stern–Volmer plots of I_0/I versus the concentration of oxygen for PS beads of two different sizes: 1.0 and 2.6 μm. Note that I_0 represents the intensity at 21% oxygen, and the emission from PtOEP at 650 nm was measured as the percentage of oxygen was gradually reduced. It is worth emphasizing that the performance of PS beads of two different sizes was essentially the same. The slope for the 1.0- and 2.6-μm beads was 0.0373 and 0.0388, respectively, suggesting that the particle size had minor influence on the oxygen response. This result is not surprising because the PS beads are relatively small in size. These latex beads are also highly porous in structure so that oxygen molecules can easily diffuse into them to quench the luminophors at approximately the same rate.

Although the current sensing system based on latexes still needs further characterization, it is believed that it should display sensing features similar to those that have been obtained for thin films [12,13]. For example, the PtOEP in PS beads has a sensitivity of ∼4% towards oxygen while the SiOEP in PS beads has no sensitivity towards oxygen. These results are essentially the same as those observed for thin films [14]. The latex-based sensors should be completely reversible. Our previous work on PtOEP-based paints suggests a drift of 0.3% per 24 h [14]. In terms of temperature dependence, the temperature dependency expressed as percent intensity change per degree is −1.15 for PtOEP and −0.34 for SiOEP, respectively. Based on these data, the temperature dependency for the ratio (I_{PtOEP}/I_{SiOEP}) can be lowered to −0.8. It is worth noting that previous work by our research group and others demonstrated no interference from water vapor, nitrogen, or carbon dioxide on the performance of PtOEP-based oxygen sensors [12,15].

4. Summary

Monodisperse PS beads loaded with SiOEP and PtOEP have been synthesized using the dispersion polymerization method. Because the number of primary particles precipitated from the reaction medium was dependent on the concentration of initiator, the sizes of these PS beads could be readily varied from 0.5 to 2.6 μm by simply controlling the concentration of initiator. The dual luminophors exhibited similar absorption spectra but two distinctive luminescent peaks with SiOEP at 580 nm and PtOEP at 650 nm. While the phosphorescence intensity of PtOEP displayed a strong dependence on the concentration of oxygen, the fluorescence of SiOEP had no response toward oxygen. A linear correlation was obtained when the luminescence intensity ratio between SiOEP at 580 nm and PtOEP at 650 nm was plotted against the concentration of oxygen. This linear dependence provides a simple, reliable, and self-referenced means to continuously monitor the concentration of oxygen.

We are currently exploring the following applications of these dual luminophor PS beads with our collaborators: (a) Lung physiology studies where 1-μm beads will be introduced into the blood stream of live animals to measure oxygen gradient during transit. The goal of this work is to produce real-time sensing of oxygen in the capillary networks of the alveoli. (b) Study of turbulence dynamics using the air-born PS beads that are small enough to follow fluid flow accurately. The goal of this work is to measure simultaneously the pressure and velocity fields. (c) Multiple luminophors, self-referenced beads are being developed to simultaneously measure both temperature and pressure.

Acknowledgements

This work has been supported in part by the Air Force Office of Scientific Research (AFOSR) through a MURI grant on Polymeric Smart Skin Materials (F49620-01-1-036) and a fellowship from the David and Lucile Packard Foundation. Y.X. is an Alfred P. Sloan Research Fellow and a Camille Dreyfus Teacher Scholar. S.H.I. has also been partially supported by the Postdoctoral Fellowship Program of the Korean Science and Engineering Foundation (KOSEF).

References

[1] H. Xu, J.W. Aylott, R. Kopelman, T. Miller, M.A. Philbert, Anal. Chem. 93 (2001) 4124–4133.

[2] K.P. McNamara, Z. Rosenzweig, Anal. Chem. 70 (1998) 4853–4859.
[3] S. Abe, K. Okamoto, H. Madarame, Meas. Sci. Technol. 15 (2004) 1153–1157.
[4] M. Gouterman, J. Callis, L. Dalton, G. Khalil, Y. Mébarki, K.R. Cooper, M. Grenier, Meas. Sci. Technol. 15 (2004) 1986–1994.
[5] J. Kavandi, J. Callis, M. Gouterman, G. Khalil, D. Wright, E. Green, D. Burns, B. McLachlan, Rev. Sci. Instrum. 61 (1990) 3340–3347.
[6] J. Harris, Ph.D. thesis, Department of Chemistry, University of Washington, 1998, pp. 22–29.
[7] Q. Ye, Z. Zhang, X. Ge, Polym. Int. 52 (2003) 707–712.
[8] J. Choi, S.-Y. Kwak, S. Kang, S.-S. Lee, M. Park, S. Lim, J. Kim, C.R. Choe, S.I. Hong, J. Polym. Sci. Part A Polym. Chem. 40 (2002) 4368–4377.
[9] A. Tuncel, R. Kahraman, E. Piskin, J. Appl. Polym. Sci. 50 (1993) 303–319.
[10] C.K. Ober, M.L. Hair, J. Polym. Sci. Part A Polym. Chem. 25 (1987) 1395–1407.
[11] O. Stern, M. Volmer, Phys. Z. 20 (1919) 183–188.
[12] G. Khalil, C. Costin, J. Crafton, S. Grenoble, M. Gouterman, J.B. Callis, L.R. Dalton, Sens. Actuators 97 (2004) 13–21.
[13] M. Gouterman, J.B. Callis, L.R. Dalton, G. Khalil, Y. Mébarki, K.R. Cooper, M. Grenier, Meas. Sci. Technol. 15 (2004) 1986.
[14] I.R. Sweet, G. Khalil, A.R. Wallen, M. Steedman, J. Reems, K. Schenkman, S. Kahn, J.B. Callis, Diabetes Technol. Therap. 4 (2002) 661.
[15] S. Dager, J. Yim, G. Khalil, A. Artra, D. Bowden, M. Kenny, Neuropsychopharmacology 12 (1995) 307.